Bioresource Technology 321 (2021) 124434

Contents lists available at ScienceDirect

Bioresource Technology

journal homepage: www.elsevier.com/locate/biortech

Light spectra as triggers for sorting improved strains of *Tisochrysis lutea*

Fengzheng Gao [a,*], Sep Woolschot [a], Iago Teles Dominguez Cabanelas [a], René H. Wijffels [a,b], Maria J. Barbosa [a]

[a] Wageningen University, Bioprocess Engineering, AlgaePARC, P.O. Box 16, 6700 AA Wageningen, Netherlands
[b] Faculty Biosciences and Aquaculture, Nord University, N-8049 Bodø, Norway

HIGHLIGHTS

- Blue light increased growth, fucoxanthin content and productivity.
- Red light decreased growth, fucoxanthin content and productivity.
- Improved strain has 16–19% higher growth and fucoxanthin productivity.
- Light spectrum does not affect total lipid and DHA content.
- Green light induced neutral lipids accumulation.

GRAPHICAL ABSTRACT

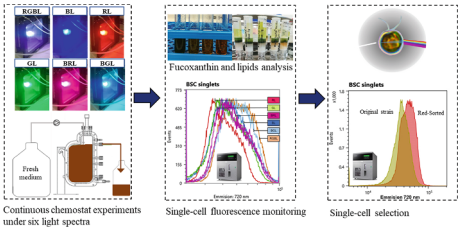

ARTICLE INFO

Keywords:
Tisochrysis lutea
Light spectra
Fucoxanthin
Lipid
Fluorescence-activated cell sorting

ABSTRACT

It is known that microalgae respond to different light colors, but not at single-cell level. This work aimed to assess if different light colors could be used as triggers to sort over-producing cells. Six light spectra were used: red + green + blue (RGBL), blue (BL), red (RL), green (GL), blue + red (BRL) and blue + green (BGL). Fluorescence-activated cell sorting method was used to analyse single-cell fluorescence and sort cells. BGL and RGBL lead to the highest fucoxanthin production, while RL showed the lowest. Therefore, it was hypothesized that hyper-producing cells can be isolated efficiently under the adverse condition (RL). After exposure to all light colors for 14 days, the top 1% fucoxanthin producing cells were sorted. A sorted strain from RL showed higher (16–19%) growth rate and fucoxanthin productivity. This study showed how light spectra affected single-cell fucoxanthin and lipid contents and productivities. Also, it supplied an approach to sort for high-fucoxanthin or high-lipid cells.

1. Introduction

Microalgae have gained high attention for the sustainable production of various compounds, such as pigments and lipids (Khan et al., 2018). Carotenoids are pigments that can be used for various purposes, such as cosmetics, pharmaceuticals, or nutraceuticals (Guedes et al., 2011). Fucoxanthin (Fx) is the main carotenoid present in brown macro- and microalgae with photosynthetic and photoprotective function (Bhattacharjya et al., 2020; Li et al., 2019), getting more and more attention due to its biological properties, such as antioxidant, anti-obesity, and antidiabetic effects (Fung et al., 2013; Maeda et al., 2018). Lipids, especially long-chain omega-3 fatty acids, such as docosahexaenoic acid (DHA), are associated with numerous health benefits in fetal development, and in cardiovascular diseases, due to an anti-inflammatory effect and a role in oxidative stress (Swanson et al., 2012). In addition to health benefits for human beings, Fx and lipids also

* Corresponding author at: Wageningen University, Bioprocess Engineering, AlgaePARC, P.O. Box 16, 6700 AA Wageningen, Netherlands.
E-mail address: fengzheng.gao@wur.nl (F. Gao).

https://doi.org/10.1016/j.biortech.2020.124434
Received 23 October 2020; Received in revised form 15 November 2020; Accepted 16 November 2020
Available online 20 November 2020

play key roles in health and development of aquatic organisms, which makes microalgae a widely used feed in aquaculture (Matsui et al., 2020; Shah et al., 2018).

Tisochrysis lutea (*T. lutea*) is a sustainable cell factory for Fx and lipid production. Fx content can reach up to 1.82% dry weight (DW) (Kim et al., 2012), which can be hundred times higher than these (0.01 to 3.7 mg/g DW) of brown seaweeds as the current Fx production feedstocks (Terasaki et al., 2012; Verma et al., 2017). In addition, the lipid content can reach up to 32% DW in this strain (Balduyck et al., 2016). Moreover, *T. lutea* can reach high specific growth rates of 0.70–1.25 d^{-1} (All et al., 2012; Tzovenis et al., 1997), which allows for rapid cell proliferation, and therefore high volumetric Fx and lipid productivities. Another characteristic that makes *T. lutea* an interesting strain is the absence of a cell wall (Wikfors and Pattersonb, 1994). Not only does this make them suited for fish feed applications due to increased digestibility, but the extractabilities of Fx and lipid are rendered more efficient as well (Kim et al., 2012). This could lead to a decrease in energy requirements in downstream processing.

In microalgae, fucoxanthin and chlorophyll *a* (chl-a) and c associate to protein resulting in a complex called FCP. (Wang et al., 2019). The absorbance spectrum of Fx ranges from 450 to 540 nm in solution (Wright and Jeffrey, 1987), but it absorbs blue-green light of wavelengths between 390 and 580 nm once it is bound in an FCP (Premvardhan et al., 2009). It can therefore be expected that most Fx producing microalgae are found in marine environments where blue-green light is prevalent. Light spectrum can affect both growth and compounds productions in microalgae (de Mooij et al., 2016; del Pilar Sánchez-Saavedra et al., 2016; Prates et al., 2018). Several studies have been done on the effect of different light spectra on the growth and biochemical composition of brown microalgae. Mouget et al. (2004) tested the influence of light spectrum and intensity on the Fx producing diatom *Haslea ostrearia*. They found that cells subjected to blue light had both higher growth rate and Fx content compared to other light spectra (white, green, yellow, red, and far-red) (Mouget et al., 2004). Similarly, according to a study by An et al. (2014), cultures of *Chaetoceros calcitrans* exposed to blue LED light also showed an increase in Fx content compared to other light spectra (white, green, red). However, the growth rate was lower than the culture grown under red light, which was accredited to the photosynthetic efficiency of photons in the red light spectrum (An et al., 2014). In addition, the increases in DHA content at blue light compared with white, red, and green light was reported in batch experiments with continuous illumination (del Pilar Sánchez-Saavedra et al., 2016). Therefore, different light spectra can be used to change the growth and pigment/lipid content in microalgae. Although Fx and lipid contents at different light spectra were reported at biomass/volumetric level, the information on Fx and lipid accumulation is still missing at single cell. In addition, in this work, light spectra treatment was applied to strain improvement, for the first time. The treatment of *T. lutea* with different light spectra can be applied as an approach to increase the productivities of Fx and lipids and potentially as selection pressure for high-Fx or high-lipid cells, which can be sorted using fluorescence-activated cell sorting (FACS).

In the present study, the effect of six light spectra on Fx and lipid accumulation in *T. lutea* was investigated in photobioreactors operated under continuous chemostat mode. Single-cell fluorescence from cells grown under different spectra were analysed using FACS. The top 1% Fx producing cells were sorted after exposure to different spectra for 14 days. This study showed how light spectra affected Fx and lipid accumulation at reactor and single cell level and supplied an approach to use light spectrum as a trigger/selection pressure for high-Fx or high-lipid cells improvement.

2. Materials & methods

2.1. Strain and maintenance conditions

T. lutea (previously identified as *Isochrysis galbana* T-Iso) (Bendif et al., 2013) and commercial culture medium stock NutriBloom Plus (Gao et al., 2020a) were kindly provided by NECTON, S.A. (Olhão, Portugal). The cultivation medium was prepared with natural seawater from the North Sea (the Netherlands) enriched with 2 mL/L of the NutriBloom Plus stock with a final pH of 8.0 (containing 20 mM HEPES). For maintenance, cultures were inoculated in 250 mL Erlenmeyer flasks with 100 mL medium. The flasks were placed in incubators (Infors, Switzerland), growing at a temperature of 25 °C, light intensity of approximately 140 μmol m^{-2} s^{-1}, 18/6h day/night cycle, 2.0% CO_2, and under constant agitation of 130 rpm.

2.2. Continuous chemostat experiment at six light spectra

Flat panel photobioreactors (Algaemist) (Hulatt et al., 2017) with a reactor volume of 400 mL were used for *T. lutea* cultivation at continuous chemostat mode with a fixed dilution rate of approximately 0.50 d^{-1}. Stirring was done by constant sparging with air, where the bubbles facilitated circulation of the liquid contents. The pH of the medium was coupled to the CO_2 supply in the air. When the pH rose above the set point of 8.0, CO_2 was added automatically to decrease the pH.

To study the effect of light spectrum on growth, Fx and lipid content and productivity of *T. lutea*, Algaemist reactors were illuminated by 50 W light-emitting diode (LED) RGB lamp (Profolux, the Netherlands) in an 18/6h day/night cycle. Six light spectra were employed in the present study: RGBL (red : green : blue ≈ 1.6:1:1.3), BL, RL, GL, BRL (blue : red ≈ 1:5) and BGL (blue : green ≈ 6:5). The wavelength of different light spectra was measured using fiber optic CCD-based spectroradiometer (AvaSpec-2048 detector, Fiber FC-IR100-1-ME, 400–700 nm, Avantes, Eerbeek, The Netherlands) (Fig. 1). The lamps were placed upright against the controlling system of the Algaemist and connected to a digital time switch. The Algaemist reactors were positioned approximately 20–25 cm from the lamp to have the same incident light intensity of 50 μmol m^{-2} s^{-1}, depending on the calibration of 28 different points on the illuminated surface for each light tested. The space between the lamp and the reactor was covered with paper to avoid interference of daylight. The reactors were operated at batch mode firstly, then switched to chemostat when the culture optical density at 750 nm (OD_{750}) reached approximately 0.7. The outgoing light intensity was measured using a light meter (LI-COR, LI250A) at the same time every day from two points evenly distributed in the middle of the back-glass panel. Overflow cultures (i.e. harvest) were collected in a 1.0 L bottle for Fx and lipid measurement.

2.3. Daily measurements

During chemostat experiments, approximately 10 mL of culture was taken from the reactor using a Luer-Lock syringe daily, approximately 30 min before the light was switched off. From this culture, OD_{750}, quantum yield (QY), cell count, and dry weight (DW) were measured according to previous reported methods (Gao et al., 2020a, 2020b). Moreover, approximately 100 mL of the harvest culture was collected and stored for cell component analysis. The harvest was distributed among two 50 mL Greiner falcon tubes. To wash the cells, the tubes were centrifuged at 15 °C and 4255 × g for 5 min. After discarding the supernatant, the cell pellets were resuspended and combined in 50 mL 0.5 M ammonium formate. The resuspended cells were centrifuged using the same centrifuge settings, after which the supernatant was discarded. Next, the cell pellets were flushed with N_2 and stored in a freezer at approximately −20 °C.

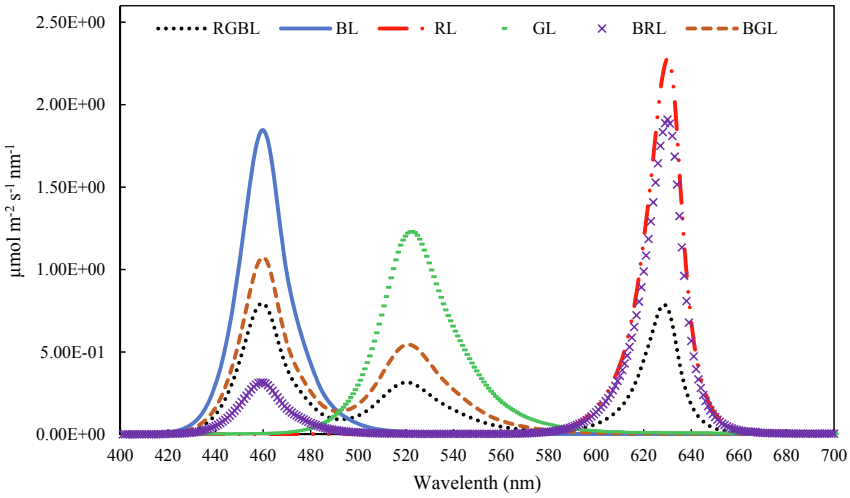

Fig. 1. Emission spectra of the LED panels Note: The curves illustrate a photon flux density of 50 μmol m^{-2} s^{-1} when integrated across the entire photosynthetically active radiation range (400–700 nm). This is the light intensity employed in the experiments.

2.4. Pigment measurement

Stored harvest samples were freeze dried (Sublimator 2 × 3 × 3–5, Zirbus Technology, the Netherlands) for pigment analysis. The 50 mL Greiner tubes containing the sample were placed on pre-cooled trays (-20 °C) after their caps were removed. The samples were freeze dried for 41 h.

To quantify the pigment content, approximately 2 mg freeze-dried sample was transferred to 2 mL lysing matrix tubes (MP Biomedicals, U.S.A.). To each tube, 1 mL of pure ethanol was added. In a beating beater (Precellys 24, Bertin Technologies, France), cells were bead beaten 3 × 60 s at 2500 rpm, with 120 s pause breaks in between, and then for 2 × 60 s after tightening the tubes. The tubes were centrifuged at 9391 × g for 1 min and the supernatant was transferred to glass tubes. This process was repeated 3 times, including bead beating 1 × 60 s between each step instead of the settings mentioned above. The glass tubes containing extract were flushed with N_2 until all ethanol had evaporated. Methanol (3 mL) was added to the dry extract, after which the solution was transferred to amber colored HPLC vials (Agilent Technologies, U.S.A.) with a 1 mL syringe equipped with a 0.2 μm Spartan™ filter head (Whatman, U.K.).

Next, the samples were prepared for analysis using High-Performance Liquid Chromatography (HPLC). The following protocol is based on the method used by Grant (2011). A Shimadzu Nexera UHPLC system (Shimadzu, Japan) was used for analysis of the samples. The instrument was equipped with a Kinetex C18 column (5 μm, 100 Å, 150 × 4.6 mm). For calibration, standards of Fx and chl-a (0, 2, 4, 6, 8, and 10 μg/mL in methanol) were prepared and analysed accordingly. Fx and chl-a were detected at a wavelength of 450 and 430 nm, respectively. Samples were injected at a volume of 20 μL. Data was processed using the appropriate software (Openlab, Agilent Technologies).

2.5. Lipid quantification

Lipids were extracted from approximately 10 mg of freeze-dried sample. To do this, 1 mL of chloroform/methanol (2:2.5 v/v) containing a weighed amount of internal standard (pentadecanoic acid (C15:0 neutral lipid) and decanoic acid (C10:0 polar lipid)) was added to 2 mL lysing matrix tubes. The cells were bead beaten twice (3 × 60 s, 120 s pause, 2500 rpm). After a 5 min cooldown of the beating, cells were bead beaten once more (2 × 60 s, 120 s pause, 2500 rpm). The contents of the tube were then transferred to heat resistant 10 mL glass tubes with 3 × 1 mL chloroform/methanol mixture with standards. The tubes were sonicated for 10 min (80 kHz), followed by addition of 2.5 mL 50 mM Tris-HCl buffer (containing 1.0 M NaCl). The tubes were sonicated again (10 min, 80 kHz) and centrifuged for 5 min (1204 × g, 15 °C). The chloroform phase was collected in a fresh tube, and the remaining liquid was washed three times with 1 mL chloroform, collecting the chloroform every time. The chloroform was then evaporated with N_2.

After extraction, polar and natural lipids were separated using a SPE column (Sep–Pak Vac Silica cartridge, 6 cc, 1000 mg, Waters). The columns were equilibrated with 10 mL hexane. Concentrated samples were resuspended in 1.5 mL hexane/diethylether (7:1 v/v) and loaded onto the column. Then, neutral lipids were eluted using 10 mL of hexane/diethylether (7:1 v/v), which was collected in a fresh glass tube. Subsequently, polar lipids were eluted with 10 mL methanol/acetone/hexane (2:2:1 v/v/v) and collected in fresh glass tubes. Polar and neutral fractions were evaporated with N_2 at 30 °C.

To detect fatty acids with gas chromatography (GC), the fatty acids were methylated. To every sample, 3 mL of methanol/sulfuric acid (95:5 v/v) was added, after which the samples were heated at 100 °C for 1 h. After cooling to room temperature, 3 mL water and 3 mL hexane was added to the samples. The samples were mixed for 15 min and centrifuged for 5 min (1204 × g, 15 °C). The hexane phase was transferred to fresh glass tubes, which was then washed with 2 mL water. The hexane phase was used for GC analysis.

An Agilent 7890 GC system (Santa Clara, CA, USA) was used to determine the lipid contents. GC vials were filled with the sample containing hexane phase and placed in the autosampler. A Supelco Nucol 25,357 column (30 m × 530 μm × 1.0 μm) was used with hexane as running solvent and helium as carrier gas (20 mL min^{-1}). Data was collected and processed with Openlab software (7890 GC).

2.6. Single-cell fluorescence measurement and cell sorting

A Sony Cell Sorter SH800S with a 100 μm microfluidics sorting chip (LE-C3210, Sony, Japan) was used for single-cell fluorescence measurement. A 488 nm laser was used to excite chl-a and Fx. A 720/60 nm bandpass filter was used to detect the emission signal of these compounds. A 1.5 mL Eppendorf tube containing the sample (OD_{750} of 0.2) was placed in the sample chamber. Cells were selected from three different density plots. Firstly, the backward scatter area (BSC-A) was

plotted against the forward scattered light area (FSC-A) to distinguish bacteria and other impurities from the microalgae (Fig. 2a). A gate was created to select only the microalgal cells. Next, the FSC corresponding to a cells' height was plotted against the FSC area to select single cells (Fig. 2b). Finally, a gate was created in a BSC height versus area plot to include all cells (Fig. 2c). The single-cell fluorescence was collected from 100 000 cells.

A selection gate was created to select cells with high emission signals (top 1%) at 720 nm from each spectrum (Fig. 2d). From the selection gate, 96 single cells were selected into a sterile 96-well plate, containing 100 µL sterile NutriBloom medium (4 mM nitrogen, pH 8.0). Each well contained 1 single cell. After incubation in a climate room for 10 days, the cells were transferred to 100 mL flasks (50 mL medium) for cultivation with similar initial OD_{750} at the same conditions as before. The cultures at exponential growth phase were measured using FACS. The strain with higher fluorescence at 720 nm than the original strain was cultivated in 3 Algaemists using continuous turbidostat at 30 °C, 300 µmol m^{-2} s^{-1} (Warm white light) (de Mooij et al., 2016), 18/6h day/night cycle, and constant biomass concentration (~0.62 g L^{-1} DW). The original *T. lutea* was cultivated in another 3 Algaemists under the same parameters. After at least 3 replacement of the cultivation volume (1200 mL) during steady state, the culture was measured using FACS again.

2.7. Data analysis

The results were analysed based on the data from at least three different cultivation points during steady state. Experimental results were expressed as mean value ± SD. Differences between groups were tested for significance by the least significant difference mean comparison using the IBM® SPSS® Statistics software program (version 25). The relationship between variables was determined by one-way ANOVA at a significance level of 0.05 using a Duncan Post-Hoc test.

The volumetric biomass productivity (P_X; g L^{-1} d^{-1}) was calculated using Eq. (1);

$$P_X = Cx \times D \quad (1)$$

where *Cx* was the biomass concentration (g L^{-1}) at steady state and D was the dilution rate (d^{-1}); and was given as an average productivity. The growth rate in continuous experiments during steady state is equal to the dilution rate D (d^{-1}) which was calculated by the ratio between the overflow culture volume and total culture volume (400 mL) inside

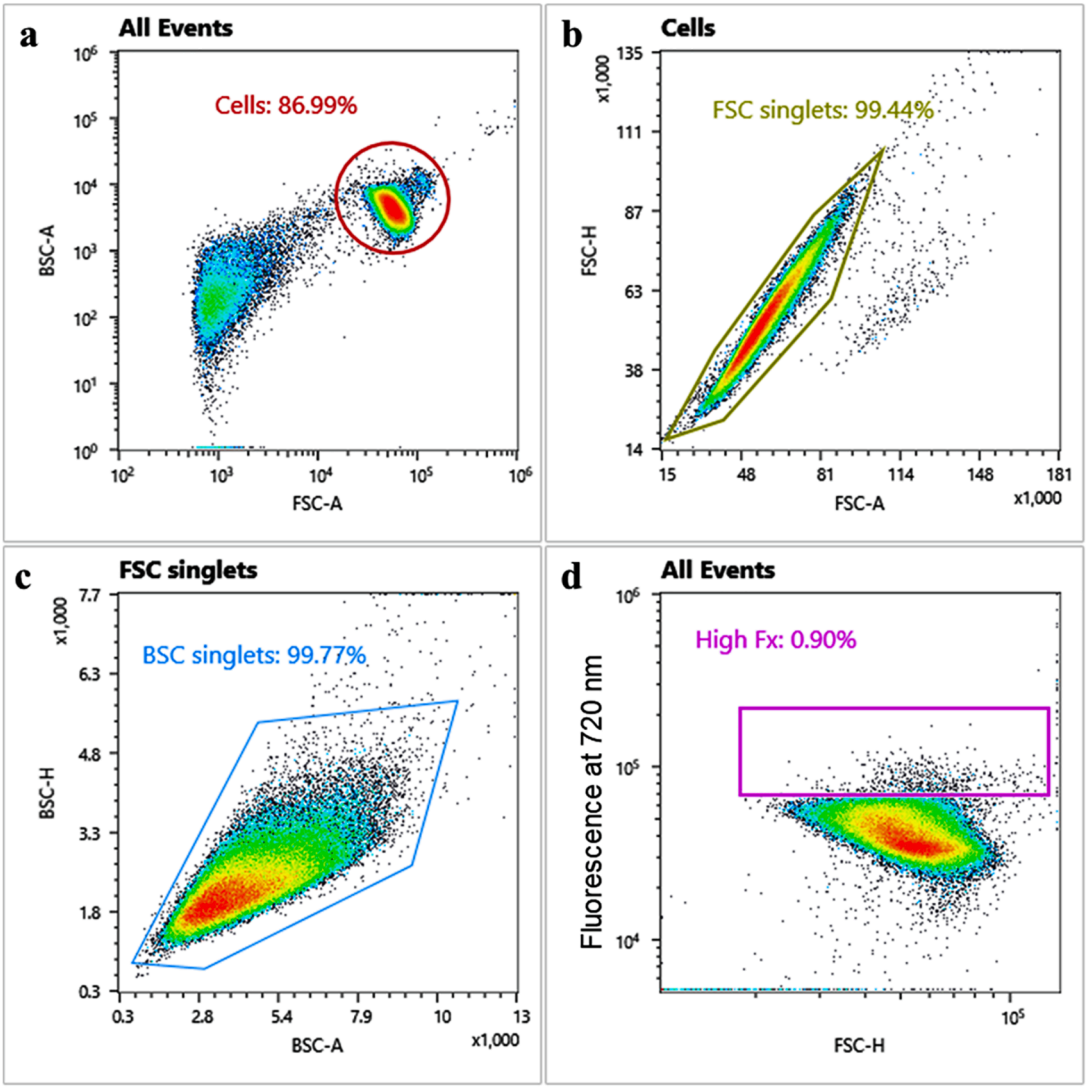

Fig. 2. Density plots as created by the Sony Cell Sorter. (a) Complexity (BSC-A) versus cell size (FSC-A) and gates that distinguish cells from bacteria; (b) Cell size height (FSC-H) versus cell size area (FSC-A) with a gate that selects singlets; (c) Complexity height (BSC-H) versus complexity area (BSC-A) to select all microalgae cells; (d) Fluorescence at 720 nm (for fucoxanthin) versus cell size FSC-H. A gate was created for high fucoxanthin-containing cells (top 1%). BSC: backward scatter area; FSC: forward scattered; A: area; H: height.

the photobioreactors.

The volumetric Fx productivity (P_{Fx}; mg L^{-1} d^{-1}) was calculated using Eq. (2);

$$P_{Fx} = C_{Fx} \times P_X \quad (2)$$

where C_{Fx} was the Fx concentration (mg g^{-1}) at steady state and P_X was the biomass productivity (g L^{-1} d^{-1}); and was given as an average productivity.

3. Results and discussion

3.1. Effects of light spectrum on growth

The exposure time to different light spectra was 14 days with steady state lasted for at least 8 days. Light spectra had a significant effect on biomass concentration and productivity of *T. lutea*. The biomass concentrations in steady state for the different spectra were: RBGL (0.38 g/L) > BGL (0.27 g/L) ≈ BL (0.25 g/L) > GL (0.17 g/L) ≈ BRL (0.15 g/L) > RL (0.07 g/L) (Table 1). The highest biomass productivity (0.17 g L^{-1} d^{-1}) was obtained at RGBL followed by BGL (0.14 g L^{-1} d^{-1}), BL (0.12 g L^{-1} d^{-1}), GL (0.09 g L^{-1} d^{-1}), BRL (0.08 g L^{-1} d^{-1}), and RL (0.04 g L^{-1} d^{-1}) (Table 1). The biomass productivity at RGBL was 4.25-fold higher than RL. These findings implied that BL on its own, or in combination with another light spectrum, affects biomass growth positively. This was corroborated by other studies, consistently reporting that blue light enhances growth by inducing DNA and RNA production in varying species of microalgae (Das et al., 2011; del Pilar Sánchez-Saavedra et al., 2016; Mouget et al., 2005; Yoshioka et al., 2012). For example, intermittent blue light (20 μmol m^{-2} s^{-1}) significantly increased biomass concentration of *I. galbana* in batch cultures (Yoshioka et al., 2012). Compared to continuous white light, and intermittent white or red-light irradiation, the cell DW was 1.5-fold higher under intermittent blue light (from 98.3 to 155 mg L^{-1}). del Pilar Sánchez-Saavedra et al. (2016) also found an increase in growth rate under continuous blue light (60 μmol m^{-2} s^{-1}) in batch cultures of *T. lutea* with respect to green and red light. They found growth rates of 1.47, 1.43, 1.23, and 1.22 d^{-1} for blue, white, red, and green light, respectively.

Yellow light resulted in the highest areal productivity which was almost double as these at blue, orange-red, and deep red lights with a fixed absorbed light (1490 μmol m^{-2} s^{-1}) in *Chlamydomonas reinhardtii* cultivation at turbidostat cultivation mode (de Mooij et al., 2016). In the present study, the incident light was the same at 50 μmol m^{-2} s^{-1}, whereas the outgoing light differed at different light spectra due to different biomass concentration during steady state and different absorption efficiency by the culture. The lowest outgoing light was found at BL and BGL while highest at RL (Table 1; $p < 0.05$). The high absorption efficiency (~93%) at BL or BGL and the low absorption efficiency (57%) at RL indicated the preferred light spectra that can be used by *T. lutea*. More time (10 days) was needed for reaching steady state at RL during continuous chemostat cultivation. Wavelengths in the blue (peak at 460 nm) and green regions (peak at 520 nm) were essential for growth of *T. lutea* due to light absorption ranges of FCP, whereas RL (peak at 630 nm) decreased biomass productivity. RL and BRL showed to be limiting growth more than RGBL, BGL, BL, and GL, which can be related to the lack of usable (i.e. blue or green) light can be absorbed by Fx. Additionally, cells at RL showed to have a significantly smaller cell size than any other lights (Table 1; $p < 0.05$). Compared to BL and BRL, the cell size was almost 1 μm (~17%) smaller in RL. Longer wavelengths like RL contain less energy, so less radical oxygen species (ROS) were formed compared to GL, BL, or a combination thereof. ROS generation has been linked to cell size before in *Chlorella vulgaris*, and ROS generation was found to be wavelength dependent (Kim et al., 2014). Moreover, RL was found to suppress genes responsible for cell division inhibition, therefore increasing cell division at an earlier stage. Expression of this particular gene was correlated to cell size, and was also dependent on the wavelength (Kim et al., 2014). Cells at BL had a significantly larger cell diameter than cells that were only treated with GL or RL, including differences of 0.5 up to 1 μm. As mentioned before, BL induces DNA and RNA synthesis, which is linked to a higher cell size (Das et al., 2011; del Pilar Sánchez-Saavedra et al., 2016; Mouget et al., 2005; Yoshioka et al., 2012).

Overall, a wide range of wavelengths (RGBL) resulted in the highest biomass productivity (0.17 g L^{-1} d^{-1}). It was shown that the lack of blue or green light resulted in lower biomass productivities. The biomass productivity at RL was between 2- to 4-fold lower than other light spectra tested.

Table 1
Growth details of continuous experiments at six light spectra.

Light treatment	RGBL	BL	RL	GL	BRL	BGL
OD_{750} (abs)	0.96 ± 0.01^{a}	0.59 ± 0.02^{d}	0.26 ± 0.04^{f}	0.68 ± 0.01^{c}	0.40 ± 0.03^{e}	0.83 ± 0.03^{b}
Outgoing light intensity (μmol m^{-2} s^{-1})	9.19 ± 1.65^{c}	3.46 ± 1.28^{d}	21.42 ± 1.54^{a}	13.12 ± 0.61^{b}	10.46 ± 0.62^{c}	3.47 ± 0.06^{d}
Cell number (×10^{6} mL^{-1})	14.91 ± 0.16^{a}	12.26 ± 1.09^{b}	9.81 ± 0.90^{c}	11.59 ± 0.67^{b}	9.74 ± 1.03^{c}	14.35 ± 1.22^{a}
DW (g L^{-1})	0.38 ± 0.02^{a}	0.25 ± 0.01^{b}	0.07 ± 0.01^{d}	0.17 ± 0.02^{c}	0.15 ± 0.01^{c}	0.27 ± 0.02^{b}
Diameter (μm)	5.74 ± 0.04^{b}	5.92 ± 0.02^{a}	4.98 ± 0.06^{d}	5.40 ± 0.11^{c}	5.96 ± 0.08^{a}	5.61 ± 0.10^{b}
QY (Fv/Fm)	0.74 ± 0.02^{ab}	0.75 ± 0.01^{ab}	0.76 ± 0.02^{a}	0.72 ± 0.01^{b}	0.75 ± 0.02^{ab}	0.73 ± 0.01^{ab}
μ (d^{-1})	0.45 ± 0.02^{d}	0.48 ± 0.01^{bc}	0.50 ± 0.01^{bc}	0.55 ± 0.01^{a}	0.54 ± 0.03^{c}	0.50 ± 0.01^{b}
Biomass productivity (g L^{-1} d^{-1})	0.17 ± 0.01^{a}	0.12 ± 0.00^{c}	0.04 ± 0.01^{e}	0.09 ± 0.01^{d}	0.08 ± 0.01^{d}	0.14 ± 0.01^{b}
Ratio Fx/Chl-a (w/w)	0.56 ± 0.01^{c}	0.67 ± 0.03^{b}	0.83 ± 0.04^{a}	0.60 ± 0.01^{c}	0.85 ± 0.03^{a}	0.59 ± 0.01^{c}

Note: values represent mean ± SD. Means with different letters are significantly different from each other (comparisons were made between groups for each variable) ($p < 0.05$).

3.2. Effect of light spectrum on fucoxanthin content and productivity

BGL resulted in the highest Fx content (1.68% DW), followed by RGBL (1.63% DW), BL (1.59% DW), BRL (1.45% DW), GL (1.37% DW), and RL (1.33% DW) (Fig. 3a). Additionally, the trends of Fx cell content (pg/cell) were similar to Fx (% DW). However, larger differences were found in Fx cell content between different lights where the highest Fx cell content at RGBL (0.42 pg/cell) was 4.2-fold higher than the lowest Fx cell content at RL (0.10 pg/cell) (Fig. 3b). Similar Fx cell contents (0.32 pg/cell) were found at BL and BGL which were higher than at BRL (0.22 pg/cell) and GL (0.20 pg/cell) (Fig. 3b).

The highest Fx content in BGL-treated cells can be expected since BGL is prevalent in the natural habitat of brown microalgae (Wang et al., 2019). A Fx content of 2.05% AFDW (ash-free DW) was found in *T. lutea* in a previous study (Ishika et al., 2017). Using the average ash content (13.5% DW) found for *T. lutea* by Bernaerts et al. (2018), the value mentioned above corresponds to approximately 1.77% DW. The Fx content was obtained at a light irradiance of 150 μmol m^{-2} s^{-1} and under high salinity (45‰). The Fx productivity was approximately 9-fold lower (0.055 mg L^{-1} d^{-1}) than the lowest productivity reached in the present study (0.49 mg L^{-1} d^{-1}; Fig. 2a). The lack of blue light resulted in a decreased Fx content in GL and RL. Wang et al. (2018) observed an upregulation of 6 proteins closely related to photosynthesis in a BL treated culture of *Cylindrotheca closterium*. In the same study it was concluded that photosynthesis and Fx production have a close connection. Moreover, BL induces ROS generation, which have to be quenched by Fx (Kim et al., 2014). As a response to BL, more Fx was produced in microalgae. In the present study, RL was considered as an

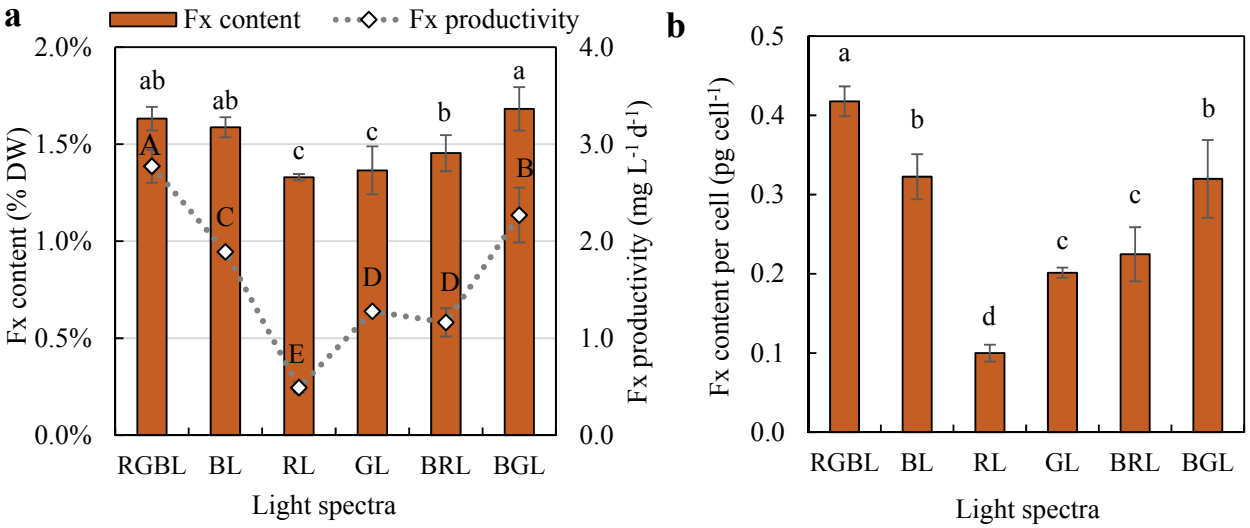

Fig. 3. Fucoxanthin content and productivity (a) and fucoxanthin cell content (b) of *T. lutea* at six light spectra Note: values are the means ± SD; Lowercase and uppercase letters represent different homogeneous subsets of significance for the fucoxanthin (cell) content and productivity ($p < 0.05$), respectively.

extreme condition for growth and Fx production of *T. lutea*. However, RL could be applied as a selection pressure in high-Fx cell selection. The cells produced more Fx at extreme condition (RL) and probably can produce high Fx at optimal conditions (RGBL or BGL).

In the present cultivation conditions, RGBL resulted in the highest Fx productivity (2.77 mg L^{-1} d^{-1}), followed by BGL (2.27 mg L^{-1} d^{-1}) > BL (1.89 mg L^{-1} d^{-1}) > GL (1.28 mg L^{-1} d^{-1}) ≈ BRL (1.16 mg L^{-1} d^{-1}) > RL (0.49 mg L^{-1} d^{-1}). The independency on RL was evident, as RL illumination resulted in the lowest Fx content and productivity. The Fx productivities at RL were 5.7 and 4.6 times lower than RGBL and BGL, respectively. The incapability of RL to induce genes responsible for carotenoid synthesis could explain the observed trend. Fx and chl-a have a high absorption at low (blue) wavelengths, hence the higher productivity under this wavelength.

The increase in the Fx to chl-a ratio suggested that there were less chl-a molecules to accept the light energy harvested by Fx under RL and BRL (Table 1). Chl-a formation was deficient in RL treated plants (Apel and Kloppstech, 1980). Moreover, RL prevented the stabilisation of light harvesting complexes (LHCs), resulting in fewer LHCs in the plastids' membranes (Apel and Kloppstech, 1980). Therefore, less light was harvested, and growth was inhibited. Still, the presence of blue, green, and red wavelengths in RGBL treated cells resulted in a higher biomass and Fx productivity. A wider range of wavelengths induces various light-dependent genes involved in growth and carotenoid synthesis, such as phytoene synthase and phytoene desaturase (Baer et al., 2016).

3.3. Single-cell fluorescence at different light spectra and cell sorting

FACS analysis allowed for high-throughput single-cell screening for Fx content, without having to extract the pigments. According to FACS, RGBL-treated cells had the highest single-cell fluorescence, followed by BGL, BL, BRL, GL, and RL (Fig. 4a). The same trend was found for the Fx cell content (Fig. 3b). A positive correlation was found between the Fx cell content and the mean fluorescence (Fig. 4b; $R^2 = 0.87$). This confirmed that FACS is a reliable tool to estimate the Fx content of single cells. The single-cell fluorescence at 720 nm can be used for Fx monitoring (Gao et al., 2020b). FACS is widely used as a tool for compound measurement and microalgal cell sorting (Cabanelas et al., 2016, 2015). Different light spectra changed distributions of single-cell fluorescence. The cells at RGBL and BL with high single-cell fluorescence at 720 nm were expected to have high Fx content. Although RL-treated cells had the lowest Fx cell content, we found that some cells (~15%) had higher single-cell fluorescence than the mean fluorescence at RGBL meaning higher Fx cell content. In addition, RL-treated cells had the lowest coefficient variation (CV; 23.6%) in single-cell fluorescence distribution compared to other light spectra (27.8–34.1%), indicating a more homogeneous population at RL. RL can be considered as an extreme adverse condition for Fx accumulation. The high-Fx cells at RL are potential candidates to produce more Fx when grown at optimal conditions such as RGBL and BGL. Therefore, two selection approaches were considered for high-Fx strain improvement [1] selecting cells with high single-cell fluorescence at optimal growing conditions such as RGBL and BGL; [2] selecting cells with high single-cell fluorescence at adverse growing conditions such as RL. The high viability of *T. lutea* single-cell after sorting using FACS was found in previous study (Gao et al., 2020b).

Single cells selected from the gate with high fluorescence (top 1%) at 720 nm were expected to produce more Fx. The cells (96 from each light spectrum) grown in flasks after incubation were measured with FACS again, showing similar performance in Fx production to original strain, except one strain sorted from RL (named as Red-Sorted). The growth rate and Fx fluorescence of Red-Sorted strain were 18.6% and 16.7% higher than the original strain during steady state in continuous turbidostat experiments with the same cultivation parameters (Fig. 4c). A clear shift towards higher fluorescence values was found from the Red-Sorted strain (Fig. 4d). The Fx productivity of the Red-Sorted strain increased 16.2%. RL showed possibilities to create new strains selected from extreme conditions, possibly increasing their industrial performance. In general, 3–5 rounds of sorting are needed for an improved mutant (Pereira et al., 2018). However, a 16–19% improvement was achieved after one round of sorting in the present work.

Directed evolution can be induced by exposition to different light spectra to obtain phenotypes with different pigmentation characteristics, without genetic manipulation. The improved performance was most probably attributed to spontaneous mutation and adaptation. The strains obtained from this method are considered non-GMO (genetically modified organisms) and can therefore be used in the food and feed industries (Eriksson et al., 2019). In general, the chance to get an improved strain from spontaneous mutation is low (0.08–10.12 × 10^{-10} mutations per nucleotide per generation) (Krasovec et al., 2018). However, FACS allowed selection and sorting of cells with high Fx (top 1%), which led to a phenotype with improved growth rate and Fx productivity. In this way, FACS accelerated the procedure to obtain an improved phenotype. Overall, light spectrum could be combined with FACS as a strategy to obtain high-Fx cells, based on single-cell

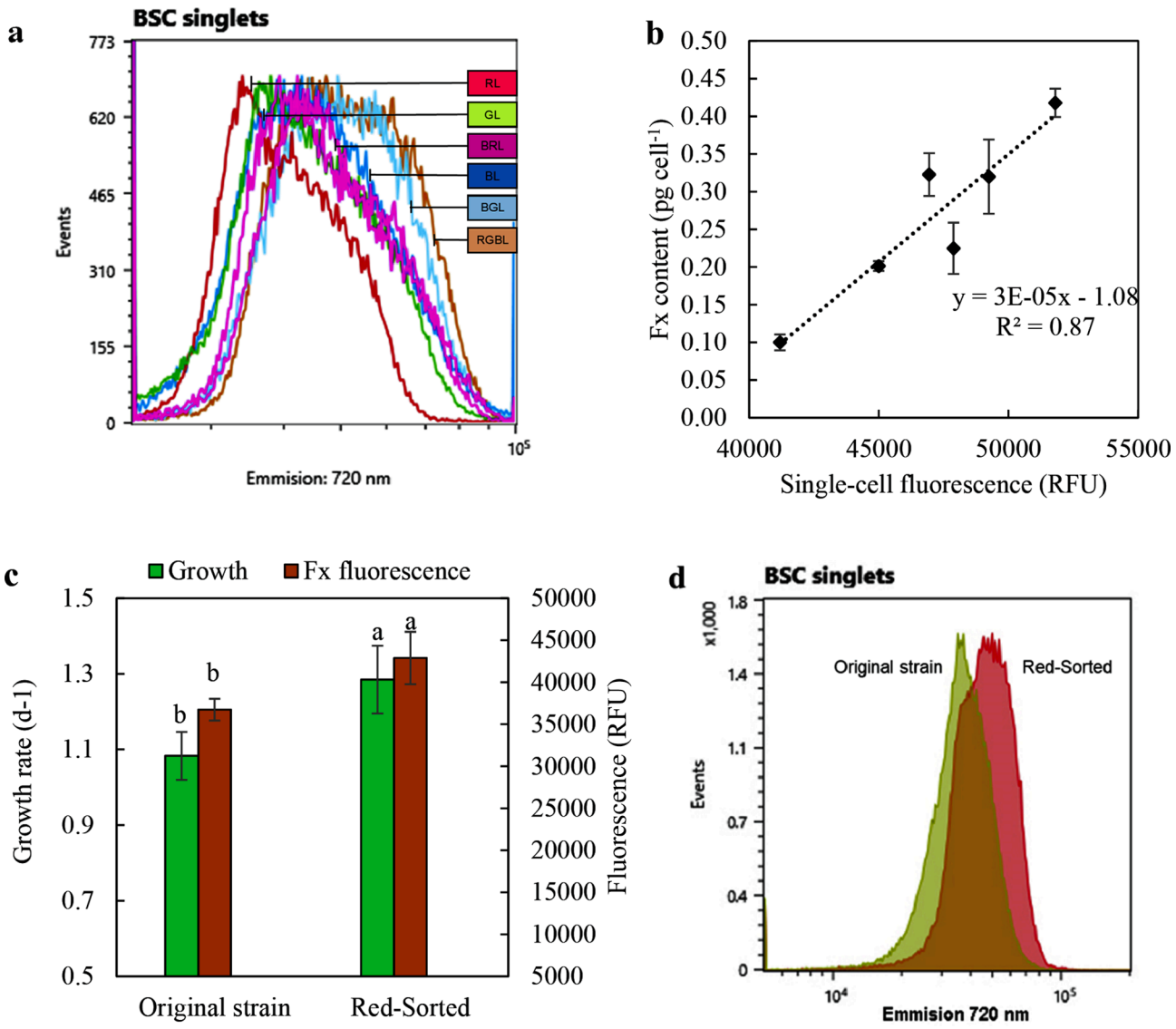

Fig. 4. Single-cell fluorescence at emission wavelength of 720 nm (a), correlation between single-cell fluorescence and fucoxanthin cell content (b), growth and fucoxanthin fluorescence of original and sorted strains (c) and single-cell fluorescence of original and sorted strains (d).

fluorescence without genetic manipulation.

3.4. Effect of light spectrum on lipid production

The composition of fatty acids in *T. lutea* can change upon varying cultivation settings (Marchetti et al., 2018). In the present study, no significant differences were found in TFA content between the light spectra (Fig. 5a; $p > 0.05$). In general, the average TFA content was 17.31–19.46% DW. This is lower than reported in previous studies, where TFA contents of 20–25% DW were found (Alkhamis and Qin, 2016; Hu et al., 2018) in *T. lutea*. The TFA productivity was in line with biomass productivity. These results are in line with the findings of Yoshioka et al. (2012), who did not observe significant differences in TFA content between various light regimes (white, red, and blue) in *T. lutea*. Although TFA didn't change at different light spectra, lipid cell content changed largely where RGBL resulted in a 3.8-fold lipid cell content as that at RL (Fig. 5b). The lipid content per cell was in line with Fx cell content, which is strongly affected by cell diameter (cell weight).

3.5. Lipid saturation and DHA production at different light spectra

In the present study, the relative content of neutral fatty acids was stable at 1.82–3.61% TFA, except for GL and BGL (Fig. 6a). Therefore, these cells were not stressed (Alishah Aratboni et al., 2019), which was also displayed by the QY (Table 1). However, the fraction of neutral fatty acids in GL and BGL was 13.69 and 13.73% TFA, respectively, while the QY was lower, but not significantly different from the rest (Fig. 6a; Table 1; $p > 0.05$).

The degrees of fatty acids saturation in *T. lutea* were similar in all light conditions (Table 2). On average, the relative amounts of saturated (SFA), monounsaturated (MUFA), and polyunsaturated (PUFA) fatty acids were 28.59, 16.91, and 54.50% TFA, respectively. The latter was especially interesting due to its high commercial value and wide applicability in food products (Draaisma et al., 2013). For comparison, a relative PUFA content of approximately 26.2% TFA was found in batch cultivation under different light spectra (60 μmol m^{-2} s^{-1}; continuous illumination) (del Pilar Sánchez-Saavedra et al., 2016). A PUFA content of 26.1% TFA was found under white light (50 μmol m^{-2} s^{-1}; 12:12 light/dark cycle) (Alkhamis and Qin, 2016). The PUFA content in the present study is the double of that found in these previous reports.

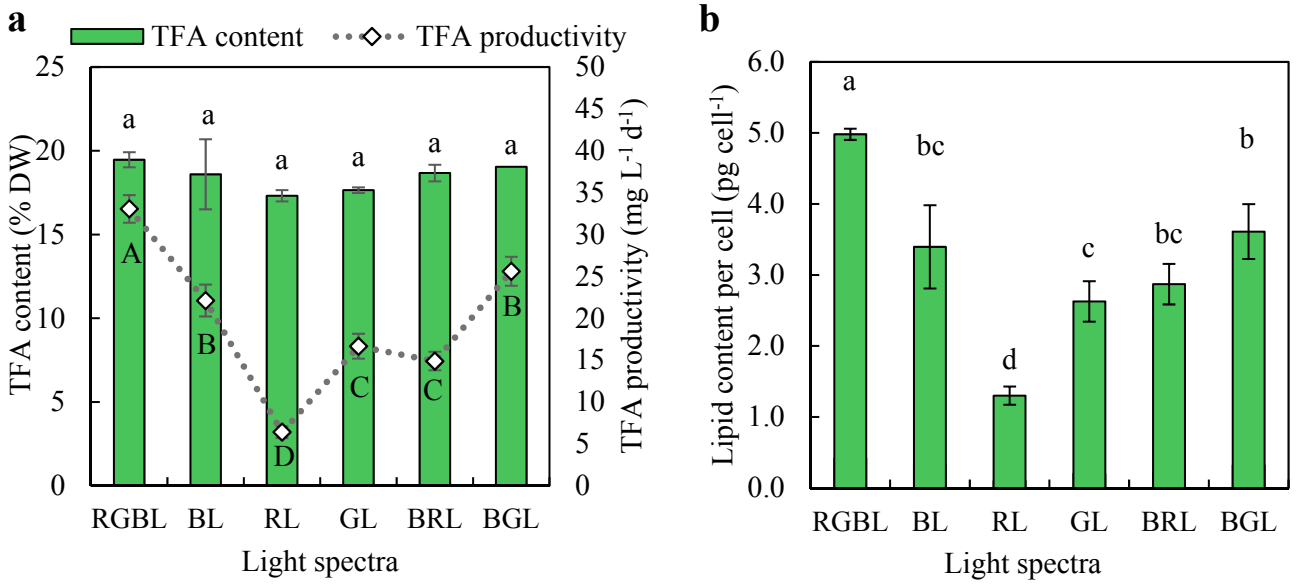

Fig. 5. Total fatty acids content and productivity (a) and lipid content per cell (b) Note: values are the means ± SD; Lowercase letters represent different homogeneous subsets of significance for total fatty acids content (a) and lipid content per cell (b) ($p < 0.05$); Uppercase letters represent different homogeneous subsets of significance for total fatty acids productivity (a) ($p < 0.05$).

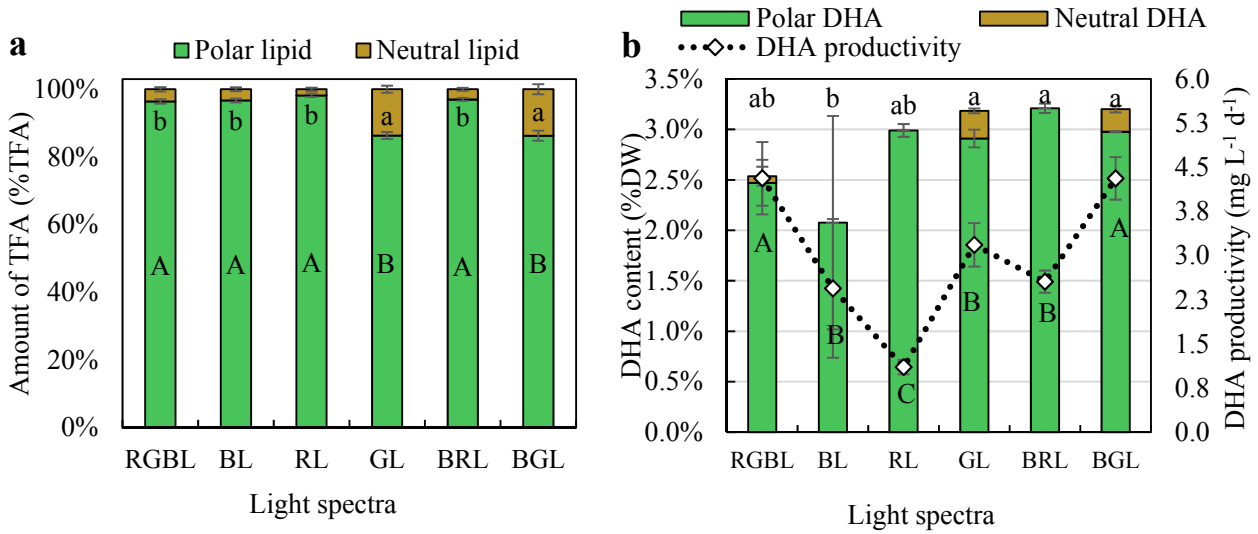

Fig. 6. The amount of polar and neutral lipid in total fatty acids (a) and DHA content and productivity (b) in *T. lutea* at six light spectra Note: values are the means ± SD; Bars with different letters are significantly different from each other; Lowercase letters represent different homogeneous subsets of significance for neutral lipid (a) and DHA content (b) ($p < 0.05$); Uppercase letters represent different homogeneous subsets of significance for polar lipid (a) and DHA productivity (b) ($p < 0.05$).

However, under white light irradiation of a batch culture (~40 μmol m^{-2} s^{-1}; 14 : 10 light/dark cycle), similar results were obtained to the present work, where a relative amount of SFAs, MUFAs, and PUFAs was reported as 30.5, 18.4, and 51.1% TFA in *T. lutea* (Hu et al., 2018). The results from these studies show that the level of saturation is independent of light spectra.

T. lutea is often characterised by its ability to accumulate high levels of DHA. In the present study, the DHA content ranged from 2.08 (BL) to 3.21% DW (BRL), and 10.70 (BL)–18.05% (GL) TFA. No significant differences in terms of DHA content were found between cells exposed to RGBL, RL, GL, BRL, and BGL (Fig. 6b; $p > 0.05$). The next lowest DHA content was found with RGBL (2.54% DW corresponded to 13.01% TFA), which was still higher than that obtained by Saoudi-Helis et al. (1994). They found DHA levels of 1.6% DW at steady-state growth, which corresponded to a DHA content of 6 – 8% TFA in *T. lutea* at a light intensity of 150 μmol m^{-2} s^{-1}. DHA content of 11.69 and 9.63% TFA were obtained in the exponential and stationary phase in batch, respectively (del Pilar Sánchez-Saavedra et al., 2016). A DHA content of 10.1%TFA was found in continuous mode, using white cool fluorescent lamps (Alkhamis and Qin, 2016). In both cases, a similar light intensity (~50 μmol m^{-2} s^{-1}) but a lower temperature (20–25 °C) was used in these studies.

In cells exposed to GL, a fraction of the DHA was found to be in the neutral lipids. RGBL-, BGL-, and GL-treated cells had a neutral DHA content of 0.07, 0.22, and 0.27% DW, respectively (Fig. 6b). These results implied that GL induces the production of neutral lipids.

Neutral lipids are commonly accepted as energy storage under adverse cultivation conditions, e.g., excessive irradiance, nutrient starvation (especially nitrogen), and temperature drops (Solovchenko, 2012). GL was channeled through the FCP by Fx when exposed to this

Table 2
Fatty acids profile of *Tisochrysis lutea* under different light spectra.

Light spectra	RGBL	BL	RL	GL	BRL	BGL
C14:0	18.50 ± 0.15^{ab}	19.26 ± 1.06^{a}	17.88 ± 0.36^{b}	16.32 ± 0.13^{c}	18.38 ± 0.20^{ab}	18.37 ± 0.8^{ab}
C16:0	9.48 ± 0.07^{b}	9.17 ± 0.56^{b}	10.52 ± 0.84^{a}	9.73 ± 0.14^{ab}	9.17 ± 0.03^{b}	8.81 ± 0.30^{b}
C18:0	0.43 ± 0.01^{ab}	0.58 ± 0.03^{ab}	1.11 ± 0.73^{a}	0.12 ± 0.17^{b}	0.49 ± 0.02^{ab}	0.20 ± 0.14^{b}
C19:0	0.50 ± 0.02^{c}	0.00 ± 0.00^{d}	0.00 ± 0.00^{d}	1.68 ± 0.09^{a}	0.00 ± 0.00^{d}	0.85 ± 0.05^{b}
∑SFA	**28.90 ± 0.19^{a}**	**29.01 ± 1.57^{a}**	**29.50 ± 1.21^{a}**	**27.85 ± 0.41^{a}**	**28.04 ± 0.17^{a}**	**28.23 ± 0.77^{a}**
C14:1 *cis*-9	1.09 ± 0.06^{a}	0.97 ± 0.10^{abc}	0.42 ± 0.30^{d}	0.76 ± 0.01^{bc}	0.74 ± 0.02^{c}	1.07 ± 0.11^{ab}
C16:1	6.02 ± 0.27^{ab}	6.55 ± 0.61^{a}	4.62 ± 0.14^{c}	5.51 ± 0.21^{ab}	5.46 ± 0.18^{ab}	5.80 ± 0.14^{ab}
C18:1	8.25 ± 0.12^{d}	9.01 ± 0.11^{c}	10.35 ± 0.06^{a}	9.06 ± 0.15^{c}	9.70 ± 0.09^{b}	8.44 ± 0.15^{d}
C20:1	2.13 ± 0.08^{a}	1.92 ± 0.20^{a}	0.00 ± 0.00^{d}	0.47 ± 0.10^{c}	1.98 ± 0.21^{a}	1.10 ± 0.12^{b}
∑MUFA	**17.49 ± 0.29^{ab}**	**18.45 ± 0.65^{a}**	**15.39 ± 0.43^{d}**	**15.81 ± 0.30^{cd}**	**17.89 ± 0.26^{b}**	**16.41 ± 0.13^{c}**
C16:2	1.66 ± 0.06^{a}	1.91 ± 0.13^{a}	1.87 ± 0.51^{a}	1.11 ± 0.01^{b}	1.72 ± 0.02^{a}	1.39 ± 0.01^{ab}
C16:3	1.02 ± 0.07^{a}	1.02 ± 0.12^{a}	0.19 ± 0.13^{b}	0.91 ± 0.04^{a}	0.91 ± 0.03^{a}	1.08 ± 0.04^{a}
C18:2	6.77 ± 0.18^{d}	7.64 ± 0.35^{c}	10.98 ± 0.48^{b}	12.58 ± 0.60^{a}	5.95 ± 0.27^{d}	10.17 ± 0.34^{b}
C18:3	13.20 ± 0.39^{b}	14.94 ± 0.43^{a}	7.11 ± 0.10^{e}	9.11 ± 0.18^{d}	13.16 ± 0.22^{b}	12.35 ± 0.16^{c}
C18:4	16.86 ± 0.48^{a}	15.70 ± 1.91^{ab}	17.70 ± 1.00^{a}	13.76 ± 0.62^{bc}	14.23 ± 0.12^{bc}	12.58 ± 0.40^{c}
C20:5-n3	1.09 ± 0.09^{a}	0.62 ± 0.44^{a}	0.00 ± 0.00^{b}	0.82 ± 0.25^{a}	0.91 ± 0.09^{a}	0.97 ± 0.21^{a}
C22:6	13.01 ± 1.38^{bc}	10.70 ± 4.23^{c}	17.27 ± 0.30^{ab}	18.05 ± 0.63^{a}	17.19 ± 0.40^{ab}	16.82 ± 0.62^{ab}
∑PUFA	**53.61 ± 0.44^{bc}**	**52.54 ± 2.22^{c}**	**55.11 ± 0.78^{ab}**	**56.34 ± 0.68^{a}**	**54.07 ± 0.23^{abc}**	**55.35 ± 0.87^{ab}**

Note: values (% in total fatty acids) represent mean ± SD. Means with different letters are significantly different from each other (comparisons were made between groups for each variable) ($p < 0.05$).

light. The formation of neutral lipids under GL indicates an excess of energy, i.e., more energy is harvested by the FCP than what is necessary to produce new biomass. This hypothesis is corroborated by the experimental conditions providing sufficient nutrients, light, and CO_2 for continuous growth.

The DHA productivity was the highest under RGBL and BGL (4.31 mg L^{-1} d^{-1}; Fig. 6b) and was significantly lower under GL, BRL, and BL (3.18, 2.56, and 2.44 mg L^{-1} d^{-1}, respectively) ($p < 0.05$). The lowest DHA productivity was found under RL (1.11 mg L^{-1} d^{-1}), which was 3.9-fold lower than the highest one. Light spectrum affected TFA and DHA productivities by affecting biomass productivity.

4. Conclusions

Six light spectra were employed to investigate single-cell Fx and lipid accumulations. BGL resulted in the highest Fx content while RGBL resulted in the highest Fx productivity. Different light spectra changed the single-cell fluorescence distributions where RL-treated cells had a more uniform population (i.e., lower variability). A sorted strain from RL showed higher growth rate and Fx content. Light spectra did not affect TFA and DHA contents. However, GL induced neutral lipids accumulation. A wilder wavelength is considered favourable for both Fx and lipid productivity. Overall, different light spectra combined with FACS could be applied to select for high-Fx/lipid strains.

CRediT authorship contribution statement

Fengzheng Gao: Investigation, Methodology, Formal analysis, Data curation, Software, Visualization, Writing - original draft, Supervision, Writing - review & editing. **Sep Woolschot:** Investigation, Formal analysis, Data curation, Writing - review & editing. **Iago Teles Dominguez Cabanelas:** Project administration, Formal analysis, Methodology, Supervision, Writing - review & editing. **René H. Wijffels:** Project administration, Supervision, Writing - review & editing. **Maria J. Barbosa:** Project administration, Formal analysis, Funding acquisition, Methodology, Supervision, Writing - review & editing.

Declaration of Competing Interest

The authors declare that they have no known competing financial interests or personal relationships that could have appeared to influence the work reported in this paper.

Acknowledgements

This research is part of the MAGNIFICENT project, funded by the Bio Based Industries Joint Undertaking under the European Union's Horizon 2020 research and innovation program (grant agreement No. 745754).

References

Alishah Aratboni, H., Rafiei, N., Garcia-Granados, R., Alemzadeh, A., Morones-Ramírez, J.R., 2019. Biomass and lipid induction strategies in microalgae for biofuel production and other applications. Microb. Cell Fact. 18, 1–17. https://doi.org/10.1186/s12934-019-1228-4.

Alkhamis, Y., Qin, J.G., 2016. Comparison of pigment and proximate compositions of *Tisochrysis lutea* in phototrophic and mixotrophic cultures. J. Appl. Phycol. 28 (1), 35–42.

All, E.B.V., Dean, L., Robert, R., Cadoret, P., Physiologie, L., Bp, Y., Marins, M., Exp, S., Sciences, L., Marines, B., Bp, Y., Bougaran, G., Iso, T., 2012. Optimizing conditions for the continuous culture of *Isochrysis* affinis *galbana* relevant to commercial hatcheries. J. Aquacult. 326–329, 106–115.

An, Heui-Chun, Bae, Jae-Hyun, Kwon, O-Nam, Park, Heum-Gi, Park, Jin-Chul, 2014. Changes in the growth and biochemical composition of Chaetoceros calcitrans cultures using light-emitting diodesLED (Light-Emitting Diode)를 이용한 미세조류 (Chaetoceros calcitrans)의 성장 및 생화학적 조성 변화. J. Korean Soc. Fish. Technol. 50 (4), 447–454.

Apel, Klaus, Kloppstech, Klaus, 1980. The effect of light on the biosynthesis of the light-harvesting chlorophyll a/b protein: Evidence for the requirement of chlorophyll a for the stabilization of the apoprotein. Planta 150 (5), 426–430.

Baer, Sascha, Heining, Martin, Schwerna, Philipp, Buchholz, Rainer, Hübner, Holger, 2016. Optimization of spectral light quality for growth and product formation in different microalgae using a continuous photobioreactor. Algal Res. 14, 109–115.

Balduyck, Lieselot, Bijttebier, Sebastiaan, Bruneel, Charlotte, Jacobs, Griet, Voorspoels, Stefan, Van Durme, Jim, Muylaert, Koenraad, Foubert, Imogen, 2016. Lipolysis in *T-Isochrysis lutea* during wet storage at different temperatures. Algal Res. 18, 281–287.

Bendif, El Mahdi, Probert, Ian, Schroeder, Declan C., de Vargas, Colomban, 2013. On the description of *Tisochrysis lutea* gen. nov. sp. nov. and *Isochrysis nuda* sp. nov. in the Isochrysidales, and the transfer of Dicrateria to the Prymnesiales (Haptophyta). J. Appl. Phycol. 25 (6), 1763–1776.

Bernaerts, Tom M.M., Gheysen, Lore, Kyomugasho, Clare, Jamsazzadeh Kermani, Zahra, Vandionant, Stéphanie, Foubert, Imogen, Hendrickx, Marc E., Van Loey, Ann M., 2018. Comparison of microalgal biomasses as functional food ingredients: focus on the composition of cell wall related polysaccharides. Algal Res. 32, 150–161.

Bhattacharjya, Raya, Kiran Marella, Thomas, Tiwari, Archana, Saxena, Abhishek, Kumar Singh, Pankaj, Mishra, Bharti, 2020. Bioprospecting of marine diatoms *Thalassiosira*, *Skeletonema* and *Chaetoceros* for lipids and other value-added products. Bioresour. Technol. 318, 124073. https://doi.org/10.1016/j.biortech.2020.124073.

Cabanelas, Iago Teles Dominguez, Zwart, Mathijs van der, Kleinegris, Dorinde M.M., Barbosa, Maria J., Wijffels, René H., 2015. Rapid method to screen and sort lipid accumulating microalgae. Bioresour. Technol. 184, 47–52.

Cabanelas, I.T.D., Van Der Zwart, M., Kleinegris, D.M.M., Wijffels, R.H., Barbosa, M.J., 2016. Sorting cells of the microalga *Chlorococcum littorale* with increased triacylglycerol productivity. Biotechnol. Biofuels 9, 1–12. https://doi.org/10.1186/s13068-016-0595-x.

Das, Probir, Lei, Wang, Aziz, Siti Sarah, Obbard, Jeffrey Philip, 2011. Enhanced algae growth in both phototrophic and mixotrophic culture under blue light. Bioresour. Technol. 102 (4), 3883–3887.

de Mooij, Tim, de Vries, Guus, Latsos, Christos, Wijffels, René H., Janssen, Marcel, 2016. Impact of light color on photobioreactor productivity. Algal Res. 15, 32–42.

del Pilar Sánchez-Saavedra, M., Maeda-Martínez, Alfonso N., Acosta-Galindo, Salvador, 2016. Effect of different light spectra on the growth and biochemical composition of *Tisochrysis lutea*. J. Appl. Phycol. 28 (2), 839–847.

Draaisma, René B, Wijffels, René H, (Ellen) Slegers, PM, Brentner, Laura B, Roy, Adip, Barbosa, Maria J, 2013. Food commodities from microalgae. Curr. Opin. Biotechnol. 24 (2), 169–177.

Eriksson, Dennis, Kershen, Drew, Nepomuceno, Alexandre, Pogson, Barry J., Prieto, Humberto, Purnhagen, Kai, Smyth, Stuart, Wesseler, Justus, Whelan, Agustina, 2019. A comparison of the EU regulatory approach to directed mutagenesis with that of other jurisdictions, consequences for international trade and potential steps forward. New Phytol. 222 (4), 1673–1684.

Fung, Adah, Hamid, Nazimah, Lu, Jun, 2013. Fucoxanthin content and antioxidant properties of *Undaria pinnatifida*. Food Chem. 136 (2), 1055–1062.

Gao, Fengzheng, Teles (Cabanelas, ITD), Iago, Wijffels, René H, Barbosa, Maria J, 2020a. Process optimization of fucoxanthin production with *Tisochrysis lutea*. Bioresour. Technol. 315, 123894. https://doi.org/10.1016/j.biortech.2020.123894.

Gao, Fengzheng, Teles (Cabanelas, ITD), Iago, Ferrer-Ledo, Narcís, Wijffels, René H., Barbosa, Maria J., 2020b. Production and high throughput quantification of fucoxanthin and lipids in *Tisochrysis lutea* using single-cell fluorescence. Bioresour. Technol. 318, 124104. https://doi.org/10.1016/j.biortech.2020.124104.

Grant, C., 2011. Light intensity influences on algal pigments, proteins and carbohydrates: implications for pigment-based chemotaxonomy. J. Chem. Inf. Model. 53, 1689–1699. https://doi.org/10.1017/CBO9781107415324.004.

Guedes, A.C., Amaro, H.M., Malcata, F.X., 2011. Microalgae as sources of carotenoids. Mar. Drugs 9, 625–644. https://doi.org/10.3390/md9040625.

Hu, Hao, Ma, Lin-Lin, Shen, Xiao-Fei, Li, Jia-Yun, Wang, Hou-Feng, Zeng, Raymond Jianxiong, 2018. Effect of cultivation mode on the production of docosahexaenoic acid by *Tisochrysis lutea*. AMB Expr. 8 (1) https://doi.org/10.1186/s13568-018-0580-9.

Hulatt, C.J., Wijffels, R.H., Bolla, S., Kiron, V., 2017. Production of fatty acids and protein by Nannochloropsis in flat-plate photobioreactors. PLoS One 12, 1–17. https://doi.org/10.1371/journal.pone.0170440.

Ishika, Tasneema, Moheimani, Navid R., Bahri, Parisa A., Laird, Damian W., Blair, Sandra, Parlevliet, David, 2017. Halo-adapted microalgae for fucoxanthin production: effect of incremental increase in salinity. Algal Res. 28, 66–73.

Khan, M.I., Shin, J.H., Kim, J.D., 2018. The promising future of microalgae: current status, challenges, and optimization of a sustainable and renewable industry for biofuels, feed, and other products. Microb. Cell Fact. 17, 1–21. https://doi.org/10.1186/s12934-018-0879-x.

Kim, Dae Geun, Lee, Changsu, Park, Seung-Moon, Choi, Yoon-E, 2014. Manipulation of light wavelength at appropriate growth stage to enhance biomass productivity and fatty acid methyl ester yield using *Chlorella vulgaris*. Bioresour. Technol. 159, 240–248.

Kim, Sang Min, Kang, Suk-Woo, Kwon, O-Nam, Chung, Donghwa, Pan, Cheol-Ho, 2012. Fucoxanthin as a major carotenoid in *Isochrysis* aff. *galbana*: characterization of extraction for commercial application. J. Korean Soc. Appl. Biol. Chem. 55 (4), 477–483.

Krasovec, Marc, Sanchez-Brosseau, Sophie, Grimsley, Nigel, Piganeau, Gwenael, 2018. Spontaneous mutation rate as a source of diversity for improving desirable traits in cultured microalgae. Algal Res. 35, 85–90.

Li, Yuelian, Sun, Han, Wu, Tao, Fu, Yunlei, He, Yongjin, Mao, Xuemei, Chen, Feng, 2019. Storage carbon metabolism of *Isochrysis zhangjiangensis* under different light intensities and its application for co-production of fucoxanthin and stearidonic acid. Bioresour. Technol. 282, 94–102.

Maeda, H., Fukuda, S., Izumi, H., Saga, N., 2018. Anti-oxidant and fucoxanthin contents of brown alga ishimozuku (*Sphaerotrichia divaricata*) from the west coast of aomori. Jpn. Mar. Drugs 16, 1–10. https://doi.org/10.3390/md16080255.

Marchetti, Julie, da Costa, Fiz, Bougaran, Gaël, Quéré, Claudie, Soudant, Philippe, Robert, René, 2018. The combined effects of blue light and dilution rate on lipid class and fatty acid composition of *Tisochrysis lutea*. J. Appl. Phycol. 30 (3), 1483–1494.

Matsui, H., Intoy, M.M.B., Waqalevu, V., Ishikawa, M., Kotani, T., 2020. Suitability of *Tisochrysis lutea* at different growth phases as an enrichment diet for Brachionus plicatilis sp. complex rotifers. J. Appl. Phycol. https://doi.org/10.1007/s10811-020-02216-y.

Mouget, Jean-Luc, Rosa, Philippe, Tremblin, Gérard, 2004. Acclimation of Haslea ostrearia to light of different spectral qualities – confirmation of 'chromatic adaptation' in diatoms. J. Photochem. Photobiol. B: Biol. 75 (1-2), 1–11.

Mouget, Jean-Luc, Rosa, Philippe, Vachoux, Christel, Tremblin, Gérard, 2005. Enhancement of marennine production by blue light in the diatom *Haslea ostrearia*. J. Appl. Phycol. 17 (5), 437–445.

Pereira, Hugo, Schulze, Peter S.C., Schüler, Lisa Maylin, Santos, Tamára, Barreira, Luísa, Varela, João, 2018. Fluorescence activated cell-sorting principles and applications in microalgal biotechnology. Algal Res. 30, 113–120.

Prates, Denise da Fontoura, Radmann, Elisângela Martha, Duarte, Jessica Hartwig, Morais, Michele Greque de, Costa, Jorge Alberto Vieira, 2018. *Spirulina* cultivated under different light emitting diodes: enhanced cell growth and phycocyanin production. Bioresour. Technol. 256, 38–43.

Premvardhan, Lavanya, Bordes, Luc, Beer, Anja, Büchel, Claudia, Robert, Bruno, 2009. Carotenoid structures and environments in trimeric and oligomeric fucoxanthin chlorophyll a/c 2 proteins from resonance Raman spectroscopy. J. Phys. Chem. B 113 (37), 12565–12574.

Saoudi-Helis, L., Dubacq, J. -P., Marty, Y., Samain, J. -F., Gudin, C., 1994. Influence of growth rate on pigment and lipid composition of the microalgaIsochrysis aff.galbana clone T.iso. J. Appl. Phycol. 6 (3), 315–322.

Shah, Mahfuzur Rahman, Lutzu, Giovanni Antonio, Alam, Asraful, Sarker, Pallab, Kabir Chowdhury, M.A., Parsaeimehr, Ali, Liang, Yuanmei, Daroch, Maurycy, 2018. Microalgae in aquafeeds for a sustainable aquaculture industry. J. Appl. Phycol. 30 (1), 197–213.

Solovchenko, A.E., 2012. Physiological role of neutral lipid accumulation in eukaryotic microalgae under stresses. Russ. J. Plant. Physiol. 59 (2), 167–176.

Swanson, D., Block, R., Mousa, S.A., 2012. Omega-3 fatty acids EPA and DHA: health. J. Adv. Nutr. 3, 1–7. https://doi.org/10.3945/an.111.000893.Omega-3.

Terasaki, Masaru, Narayan, Bhaskar, Kamogawa, Hiroyuki, Nomura, Masatoshi, Stephen, Nimish Mol, Kawagoe, Chikara, Hosokawa, Masashi, Miyashita, Kazuo, 2012. Carotenoid profile of edible japanese seaweeds: an improved HPLC method for separation of major carotenoids. J. Aquatic Food Prod. Technol. 21 (5), 468–479.

Tzovenis, I., De Pauw, N., Sorgeloos, P., 1997. Effect of different light regimes on the docosahexaenoic acid (DHA) content of *Isochrysis* aff. *galbana* (clone T-ISO). Aquac. Int. 5, 489–507. https://doi.org/10.1023/A:1018349131522.

Verma, Priyanka, Kumar, Manoj, Mishra, Girish, Sahoo, Dinabandhu, 2017. Multivariate analysis of fatty acid and biochemical constitutes of seaweeds to characterize their potential as bioresource for biofuel and fine chemicals. Bioresour. Technol. 226, 132–144.

Wang, S., Verma, S.K., Hakeem Said, I., Thomsen, L., Ullrich, M.S., Kuhnert, N., 2018. Changes in the fucoxanthin production and protein profiles in *Cylindrotheca closterium* in response to blue light-emitting diode light. Microb. Cell Fact. 17, 1–13. https://doi.org/10.1186/s12934-018-0957-0.

Wang, Wenda, Yu, Long-Jiang, Xu, Caizhe, Tomizaki, Takashi, Zhao, Songhao, Umena, Yasufumi, Chen, Xiaobo, Qin, Xiaochun, Xin, Yueyong, Suga, Michihiro, Han, Guangye, Kuang, Tingyun, Shen, Jian-Ren, 2019. Structural basis for blue-green light harvesting and energy dissipation in diatoms. Science 363 (6427), eaav0365. https://doi.org/10.1126/science:aav0365.

Wikfors, G.H., Pattersonb, G.W., 1994. AquaCUltuVe differences in strains of kwchryszk of importance to mariculture. Aquaculture 123, 127–135.

Wright, SW, Jeffrey, SW, 1987. Fucoxanthin pigment markers of marine phytoplankton analysed by HPLC and HPTLC. Mar. Ecol. Prog. Ser. 38, 259–266.

Yoshioka, Miwa, Yago, Takahide, Yoshie-Stark, Yumiko, Arakawa, Hisayuki, Morinaga, Tsutomu, 2012. Effect of high frequency of intermittent light on the growth and fatty acid profile of *Isochrysis galbana*. Aquaculture 338-341, 111–117.